Response to Reviewers

We thank the reviewer for the constructive comments and suggestions. As suggested, we have added some details to make our analysis easier to follow and we hope our point-to-point response to the comments given below can address these concerns. The comments, our replies, and the corresponding changes in the manuscript and supplementary information are marked in black, blue, and green, respectively.

1) It looks to me that most of revisions were not made on the text or SI, though the authors tried to include additional figures to address comments in their response. I would like these figures to be included in revised manuscript.

Response: The previous changes made in the manuscript and supplement are marked in orange. Please note that in the following replies, the acronym SA stands for sulfuric acid, which has also been defined in the manuscript.

As suggested, Fig. 6 (b) and the corresponding illustration have been additionally added in the revised manuscript:

"Fig. 6 (b) shows that the particle nucleation rates (J) in the nighttime and the daytime roughly fall on the same line. Especially, the daytime values agree well with those from previous observations in Shanghai and CLOUD chamber SA-DMA (dimethylamine)-H_2O experiment. The similar J – SA relationship between the nighttime and the daytime suggests a similar nucleation mechanism as SA-base clustering. Lei Yao et al. proposed that in urban megacities, high concentration of DMA together with SA were enough to explain the particle growth to ~3 nanometers (Yao et al., 2018). Therefore, the formation of nighttime as well as daytime sub-3nm particles at our site was more likely a result of SA-DMA-H_2O nucleation." (Line 284-289, Page 11)

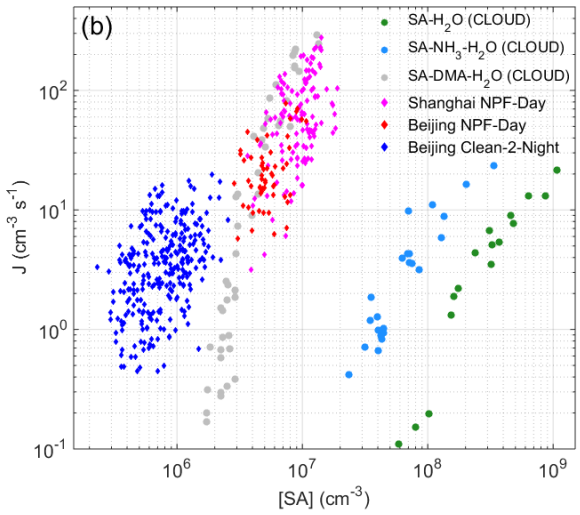

Fig. 6 (b) Comparison of Beijing ambient, Shanghai ambient and CLOUD experimental cluster formation rates against SA concentration. Green, light blue and grey dots denote CLOUD $J_{1.7}$ data for SA-H_2O, SA-NH_3-H_2O and SA-DMA-H_2O nucleation respectively (Almeida et al., 2013;Kirkby et al., 2011). Magenta diamonds represent Shanghai NPF $J_{1.7}$ data (Yao et al., 2018). Red and blue diamonds are Beijing $J_{1.5}$ data for NPF day (10:00-14:00) and Clean-2 night (20:00-04:00), respectively.

Besides, Fig. S9 and Table S5 have also been added to the revised supplement with the following explanation being added in the revised manuscript:

"Besides, João Almeida et al. suggested that when SA concentration doesn't exceed 3.0×10^7 cm^{-3}, the level of amines above 5 ppt are sufficient to reach the rate limit for amine ternary nucleation (Almeida et al., 2013). Although the median nighttime concentration of C2 amines (very likely DMA) was around 2.4 ppt (Fig. S9 and Table S5), there were also other base species (e.g., C3-amines, NH_3) co-existing. Altogether, they are sufficient to stabilize SA clusters. (Line 289-293, Page 11)

Please also note that Fig. 6 now is Fig. 6 (a).

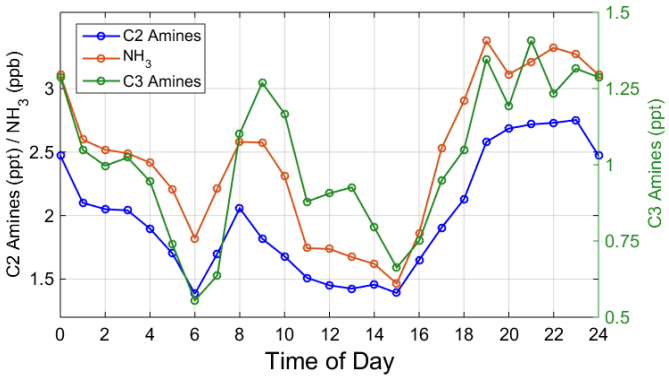

Fig. S9 Median diurnal variation of NH_3, C2 amines and C3 amines from 10th December, 2018 to 6th January, 2019.

Table S5 Median concentrations of NH_3, C2 amines and C3 amines from 10th December 2018 to 6th January 2019.

Species	Unit	Night (20:00-04:00)	Polluted Night (Vis < 12 km)	Clean-2 Night (Vis ≥ 16km, $[O_3]$ ≥ 2×10^{11} cm^{-3})
NH_3	Mixing ratio in ppb	2.8	3.3	1.9
	Concentration in cm^{-3}	7.6×10^{10}	8.9×10^{10}	5.1×10^{10}
C2 Amines	Mixing ratio in ppt	2.4	2.6	1.6
	Concentration in cm^{-3}	6.3×10^{7}	7.0×10^{7}	4.4×10^{7}
C3 Amines	Mixing ratio in ppt	1.2	1.4	0.74
	Concentration in cm^{-3}	3.1×10^{7}	3.9×10^{7}	2.0×10^{7}

2) Also, in a new ESTLett paper that came out recently (https://pubs-acs-org.elib.uah.edu/doi/10.1021/acs.estlett.0c00615), the authors showed SO3 formation (hence, sulfuric acid and even sub-3 nm particles) during the night due to heterogeneous reactions of SO2 on soot particles. Then the steady state of sulfuric acid must include this production route as well.

Response: Thanks a lot for your suggestion.

The ambient SO_3 was indeed observed. We first look into the correction between the measured concentrations of SO_3 and SA. As shown in Fig. S10 (a), under Clean-2 condition when the oxidation from alkenes ozonolysis pathway dominates the formation of SA, there is almost no apparent correlation between SA and SO_3. With the increase of pollution level, the positive correlation shows up. Under polluted condition, high aerosol surface could favor the heterogeneous production of SO_3, which might, at least to some extent, explain the extra SA sources. For this reason, we mentioned in the manuscript that there could be additional sources of SA under polluted condition.

It should be pointed out that, by assuming the pseudo-steady state, we calculated the concentration of SA based on the measured SO_3 data:

$$k_6[SO_3][H_2O]^2 = [SA]CS + \beta[SA]^2$$

where k_6=3.9×10^{-41} exp(6830.6/T) cm^{-6} s^{-1} (Jayne et al., 1997). The calculated SA concentration was over 10 times higher than the measured one. As mentioned in the ESTLett paper, "SO_3 concentration could be overestimated because the influence of ambient ions (i.e., $SO_3 \cdot NO_3^-$) was not excluded and some of the hydrate complex intermediate ($SO_3 \cdot H_2O$) also could be detected as $SO_3 \cdot NO_3^-$ ". This means that not all measured SO_3 molecules/clusters were the ones producing SA. Due to the remaining uncertainties in the measured SO_3 concentration and the unclear mechanism of the SO_2 heterogeneous pathway, we are not able to quantify the formation of SO_3 and SA from the heterogeneous reactions of SO_2 on soot particles. Therefore, we can't include this SO_2 heterogeneous term in the production of SA.

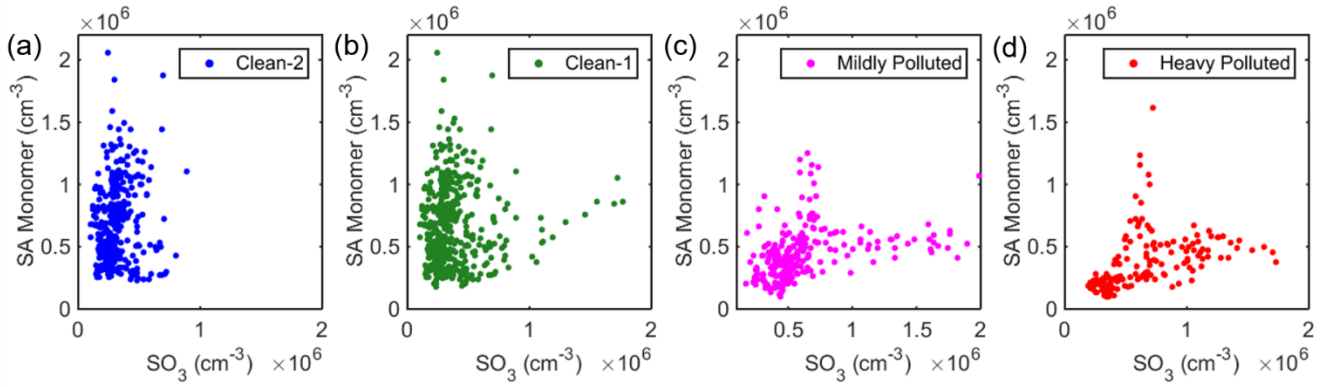

Fig. S10 Correlation between sulfuric acid monomer and SO_3 measured by CI-APi-TOF during nighttime (20:00 – 04:00 next day) from 18th January to 15th March 2019 for (a) Clean-2 condition with visibility larger than 16.0 km and O_3 concentration higher than 2.0×10^{11} cm^{-3} (~ 7 ppb), (b) Clean-1 condition with visibility larger than 12.0 km, (c) mildly polluted condition with visibility in the range of 4.0 - 12.0 km, and (d) heavy polluted condition with visibility smaller than 4.0 km.

To clarify this consideration, we added Fig. S10 in the revised supplement and the following interpretation in the revised manuscript:

"Besides, a recent study shows that SO_3 generated from the reaction of SO_2 on the surface of soot particles potentially leads to the formation of SA during nighttime and early morning (Yao et al., 2020). However, the correlation between the nighttime SA and SO_3 was only found during polluted periods (Fig. S10), suggesting that it might have an important contribution during polluted cases. This may, at least to some extent, explain the extra SA sources under polluted condition. (Line 256-260, Page 10)

3) Nevertheless, a simple 0-D box model simulations will be most useful.

Response: Thanks for your suggestion.

As suggested, the MCMv3.3.1 was used to simulate the production rate of SA (P_{SA}) from the alkenes ozonolysis route. In total, 26 VOCs, including 6 alkenes, and 5 trace gases were added as input parameters (Table R1). It should be noted that the isomers of VOCs molecules cannot be distinguished due to the lack of structure information, and fractions of different isomers

were roughly set to be equal. Both the sCI and OH pathways were simulated and their production reactions are listed in Table R2 and Table R3.

Fig. R2 shows that the median values of P_{SA} for all nights (20:00-04:00) and Clean-2 nights during the measurement period (from 18th January to 16th March 2019) are 1.61×10^{4} cm^{-3} s^{-1} and 6.07×10^{3} cm^{-3} s^{-1} respectively. As mentioned in the manuscript, the rate constant between stabilized Criegee intermediate (sCI) and SO_2 ($k_{sCI\text{-}SO_2}$) spans over several orders of magnitude, from 7.0×10^{-14} cm^3 s^{-1} (MCMv3.3.1) to 4.0×10^{-11} cm^3 s^{-1} (Ahrens et al., 2014). As expected, with the increase of $k_{sCI\text{-}SO_2}$, the modelled P_{SA} also increases dramatically, varying from 2.73×10^{3} cm^{-3} s^{-1} to 5.61×10^{4} cm^{-3} s^{-1}. Although a uniform $k_{sCI\text{-}SO_2}$ can be adjusted to match the measured SA values, but it also reflects a large uncertainty of the model. Besides, there exist large deviations between the modelled and measured concentrations of SA, with daytime SA exceedingly higher than the measured one no matter what $k_{sCI\text{-}SO_2}$ value is chosen (Fig. R3), which further reveals the uncertainty in modeling P_{SA} and SA concentration. Therefore, we still feel it is unnecessary to add the box model results in this study. However, we did mention in the manuscript that "A well-tuned box model is a useful tool to resolve it and verify the role of the ozonolysis of alkenes on the nighttime SA formation. However, such a modeling work is not included in our study, as the lacking of a complete VOC datasets and the large uncertainties in yields of sCI and oxidation rate constants of SO_2 by sCI have posed challenges in ensuring the precision of the box-model.". (Line 266-269, Page 10)

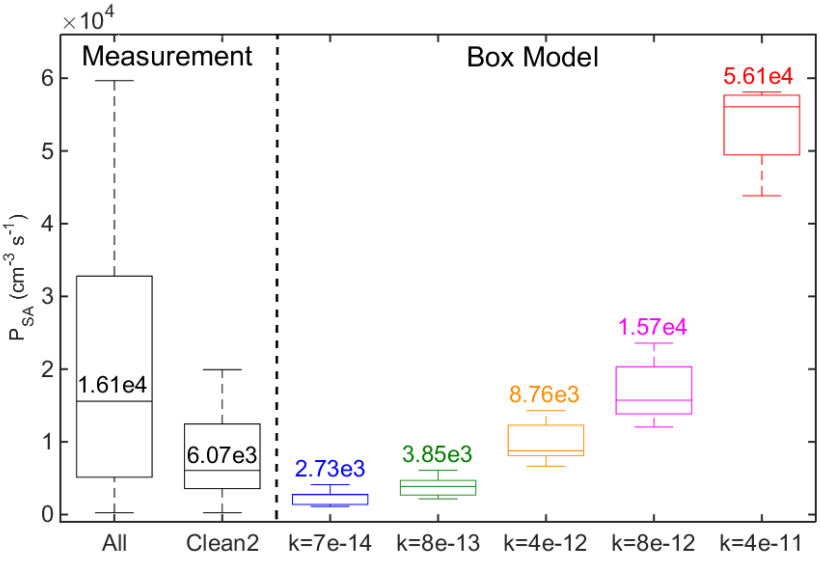

Fig. R2 Production rate of SA (P_{SA}) from measurement and box model simulation. The 'All' and 'Clean2' represent dataset belonging to all night and clean-2 night. The 'k=7e-14', 'k=8e-13', 'k=4e-12', 'k=8e-12', and 'k=4e-11' are the reaction rate constants between sCI and SO_2 with unit of cm^3 s^{-1}. The rate constant of 7.0×10^{-14} cm^3 s^{-1} is chosen from MCMv3.3.1 as a lower limit. The rate constants of 8.0×10^{-13} cm^3 s^{-1} and 4.0×10^{-11} cm^3 s^{-1} are taken from literature (Mauldin et al., 2012;Ahrens et al., 2014) and latter one is regarded as the upper limit. The middle two 4.0×10^{-12} cm^3 s^{-1} and 8.0×10^{-12} cm^3 s^{-1} are used for sensitivity analysis for the box model. The black and colored values are the corresponding median values of P_{SA}.

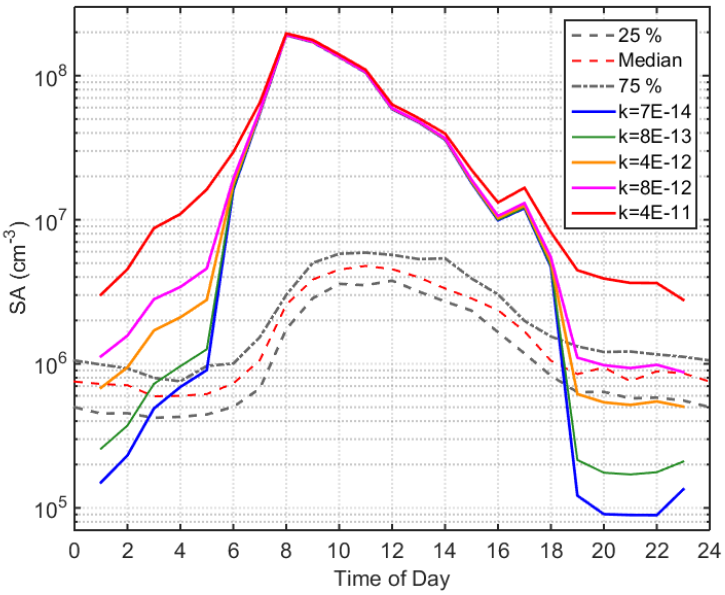

Fig. R3 Diurnal variations of measured and modelled SA concentration. The grey dashed line, red dashed line and grey dot-dashed line represent the 25 %, median and 75 % values of measured SA concentrations. The blue, green, orange, magenta and red solid lines are simulated SA concentrations from box model with different values of $k_{sCI\text{-}SO_2}$ with unit of $cm^3\ s^{-1}$.

Table R1 Input VOCs and trace gases for box model simulation

Group	Name of Species	Formula
Trace Gases	Sulfur Dioxide	SO_2
	Ozone	O_3
	Carbon Monoxide	CO
	Nitrogen Dioxide	NO_2
	Nitric Oxide	NO
Alkenes	Propylene	C_3H_6
	Butadiene	C_4H_6
	Butene	C_4H_8
	Isoprene	C_5H_8
	Pentene	C_5H_{10}
	Hexene	C_6H_{12}
Other VOCs	Butane	C_4H_{10}
	Acetone	C_3H_6O
	Pentane	C_5H_{12}
	Methyl Ethyl Ketone	C_4H_8O
	Hexane	C_6H_{14}
	Methylcyclohexane	C_7H_{14}
	Heptane	C_7H_{16}
	Octane	C_8H_{18}
	Nonane	C_9H_{20}
	Decane	$C_{10}H_{22}$
	Undecane	$C_{11}H_{24}$
	Dodecane	$C_{12}H_{26}$

Benzene	C_6H_6
Toluene	C_7H_8
Styrene	C_8H_8
Xylene	C_8H_{10}
Ethylbenzene	C_8H_{10}
Trimethylbenzene	C_9H_{12}
Ethyltoluene	C_9H_{12}
Propylbenzene	C_9H_{12}

Table R2 Production reactions of Criegee intermediate

Species	Formula	Reactions
Propylene	C_3H_6	$O_3 + C_3H_6 = CH_2OOB + CH_3CHO$ $O_3 + C_3H_6 = CH_3CHOOA + HCHO$
Butadiene	C_4H_6	$O_3 + C_4H_6 = ACR + CH_2OOD$ $O_3 + C_4H_6 = HCHO + ACROOA$
1-Butene Trans-2-Butene Cis-2-Butene	C_4H_8	$BUT1ENE + O_3 = CH_2OOB + C_2H_5CHO$ $BUT1ENE + O_3 = C_2H_5CHOOA + HCHO$ $TBUT2ENE + O_3 = CH_3CHO + CH_3CHOOB$ $CBUT2ENE + O_3 = CH_3CHO + CH_3CHOOB$
Isoprene	C_5H_8	$O_3 + C_5H_8 = CH_2OOE + MVK$ $O_3 + C_5H_8 = CH_2OOE + MACR$ $O_3 + C_5H_8 = HCHO + MVKOOA$ $O_3 + C_5H_8 = HCHO + MACROOA$
1-Pentene Trans-2-Pentene Cis-2-Pentene	C_5H_{10}	$PENT1ENE + O_3 = CH_2OOB + C_3H_7CHO$ $PENT1ENE + O_3 = C_3H_7CHOOA + HCHO$ $TPENT2ENE + O_3 = C_2H_5CHOOB + CH_3CHO$ $TPENT2ENE + O_3 = CH_3CHOOB + C_2H_5CHO$ $CPENT2ENE + O_3 = CH_3CHOOB + C_2H_5CHO$ $CPENT2ENE + O_3 = C_2H_5CHOOB + CH_3CHO$
Hexene	C_6H_{12}	$HEX1ENE + O_3 = C_4H_9CHO + CH_2OOB$ $HEX1ENE + O_3 = HCHO + NC_4H_9CHOOA$

Table R3 Production reactions of stabilized Criegee intermediate (sCI) and OH radical

Species	Production Reactions of sCI	Production Reactions OH radical
CH_2OOB	$CH_2OOB = CH_2OO$	$CH_2OOB = HO_2 + CO + OH$
CH_2OOD	$CH_2OOD = CH_2OO$	$CH_2OOD = HO_2 + CO + OH$
CH_2OOE	$CH_2OOE = CH_2OO$	$CH_2OOE = HO_2 + CO + OH$
ACROOA	ACROOA = ACROO	$ACROOA = HO_2 + CO + HCHO + CO + OH$
MVKOOA	MVKOOA = MVKOO	$MVKOOA = OH + MVKO_2$
MACROOA	MACROOA = MACROO	$MACROOA = OH + CO + CH_3CO_3 + HCHO$
CH_3CHOOA	$CH_3CHOOA = CH_3CHOO$	$CH_3CHOOA = CH_3O_2 + CO + OH$
CH_3CHOOB	$CH_3CHOOB = CH_3CHOO$	$CH_3CHOOB = CH_3O_2 + CO + OH$
C_2H_5CHOOA	$C_2H_5CHOOA = C_2H_5CHOO$	$C_2H_5CHOOA = C_2H_5O_2 + CO + OH$
C_2H_5CHOOB	$C_2H_5CHOOB = C_2H_5CHOO$	$C_2H_5CHOOB = C_2H_5O_2 + CO + OH$

C_3H_7CHOOA	$C_3H_7CHOOA = C_3H_7CHOO$	$C_3H_7CHOOA = NC_3H_7O_2 + CO + OH$
NC_4H_9CHOOA	$NC_4H_9CHOOA = NC_4H_9CHOO$	$NC_4H_9CHOOA = NC_4H_9O_2 + CO + OH$

4) It is still not clear to me how the authors retrieved the equation in Line 218 (main text) – I would like the authors to show the derivation of this equation.

$$k_{app}[Alkene][O_3][SO_2]=[SA]CS+\beta[SA]^2 \quad \text{(Line 218 in the main text)}$$

Response: Since the detailed sources of SA in the real atmosphere is really complex, e.g., the varied role of each alkene in producing OH radical, sCI, and SA, we did not intend to precisely calculate the P_{SA} from each of these individual sources. But instead, we use an approximation as indicated by the equation. As mentioned in the manuscript, the two terms on the right side denote the sink of SA, i.e., the condensation of SA onto particles and the collision of SA monomers with each other to form SA dimers. The term on the left side is an empirical one that accounts for the formation from the ozonolysis-of-alkenes-initiated oxidation of SO_2. Here, both the OH radical produced from the decomposition of Criegee intermediate (CI) (R3) and stabilized Criegee intermediate (sCI) (R2) are potentially important for oxidizing SO_2. As such oxidation is very complicated and reaction dynamics are largely unknown, precise calculation of different reactions is impossible. Therefore, we apply an empirical parameter, i.e., apparent reaction constant (k_{app}) to show the general rate of all reactions. The derivation of k_{app} is shown below.

The non-photochemical oxidation pathway for SO_2 to form SA mainly includes the following reactions (which have been listed in the manuscript, Line 75, 77, 80-83, Page 3):

$$Alkene+O_3 \xrightarrow{k_1} \varphi sCI+(1-\varphi)CI+RCHO \qquad R1$$

$$sCI+SO_2 \xrightarrow{k_2} SO_3+RCHO \qquad R2$$

$$CI \xrightarrow{k_3} OH+R_1COR_2 \qquad R3$$

$$SO_2+OH \xrightarrow{k_4} HSO_3 \qquad R4$$

$$HSO_3+O_2 \xrightarrow{k_5} SO_3+HO_2 \qquad R5$$

$$SO_3+2H_2O \xrightarrow{k_6} H_2SO_4+H_2O \qquad R6$$

where k_i is the rate constant of each reaction, φ is the yield of sCI in the ozonolysis of alkenes, and CI is the chemically activated Criegee intermediate. Besides, there are four additional reactions concerning the loss of sCI, CI and OH:

$$sCI+X \xrightarrow{k_{XX}} \dots \qquad R7$$

$$sCI \xrightarrow{k_X} \dots \qquad R8$$

$$CI \xrightarrow{k_Y} \dots \qquad R9$$

$$Z+OH \xrightarrow{k_{ZZ}} \dots \qquad R10$$

where k_{XX} is the bimolecular reaction constant for sCI with other species except from SO_2, k_X is the decomposition rate of sCI, k_Y is the deposition rate of CI which do not generate OH, and k_{ZZ} is the bimolecular constant reaction for OH with other species excluding SO_2.

Then the net production rate of SA can be expressed as:

$$P_{SA}=k_6[SO_3][H_2O]^2 \quad (1)$$

sCI, CI, OH, SO_3 and HSO_3 are short-lived intermediates, so that a PSS assumption can be applied. PSS equations for sCI, CI, OH, SO_3 and HSO_3 are as follows:

$$\text{sCI:} \quad k_1[\text{Alkene}][O_3]\varphi=k_2[\text{sCI}][SO_2]+k_{XX}[\text{sCI}][X]+k_X[\text{sCI}] \quad (2)$$

$$\text{CI:} \quad k_1[\text{Alkene}][O_3](1-\varphi)=k_3[\text{CI}]+k_Y[\text{CI}] \quad (3)$$

$$\text{OH:} \quad k_3[\text{CI}]=k_4[SO_2][\text{OH}]+k_{ZZ}[Z][\text{OH}] \quad (4)$$

$$SO_3: \quad k_2[\text{sCI}][SO_2]+k_5[HSO_3][O_2]=k_6[SO_3][H_2O]^2 \quad (5)$$

$$HSO_3: \quad k_4[SO_2][\text{OH}]=k_5[HSO_3][O_2] \quad (6)$$

then, the concentrations of sCI, CI and OH are calculated as:

$$[\text{sCI}]=\frac{k_1[\text{Alkene}][O_3]\varphi}{k_2[SO_2]+k_{XX}[X]+k_X} \quad (7)$$

$$[\text{CI}]=\frac{k_1[\text{Alkene}][O_3](1-\varphi)}{k_3+k_Y} \quad (8)$$

$$[\text{OH}]=\frac{k_3[\text{CI}]}{k_4[SO_2]+k_{ZZ}[Z]} \quad (9)$$

bring (5), (6), (7), (8) and (9) to (1) gives:

$$\begin{cases} P_{SA} = k_{app}[\text{Alkene}][O_3][SO_2] \\ k_{app} = k_1k_2\varphi\tau_{sCI}+k_1k_4(1-\varphi)\tau_{OH}\dfrac{k_3}{k_3+k_Y} \\ \tau_{sCI} = \dfrac{1}{k_2[SO_2]+k_{XX}[X]+k_X} \\ \tau_{OH} = \dfrac{1}{k_4[SO_2]+k_{ZZ}[Z]} \end{cases} \quad (10)$$

The first term and second term for k_{app} in equation (10) represent the sCI and non-photochemical OH oxidation pathways respectively. k_1, k_2 and k_4 are chosen to be 1.29×10^{-17} cm^3 s^{-1}, 8.0×10^{-13} cm^3 s^{-1}, and 1.38×10^{-12} cm^3 s^{-1} separately according to previous studies (Sipila et al., 2014;Mauldin et al., 2012;Wine et al., 1984). $\frac{k_3}{k_3+k_Y}$ is the fraction of CI decomposition leading the formation of OH radical, which is around 0.4 according to MCMv3.3.1. τ_{sCI} and τ_{OH} are the lifetimes of sCI and OH radical respectively.

It can be seen that k_{app} is highly environment-dependent, as k_{app} is not only influenced by the yields of OH radical and sCI, but also determined by the rate constants of various reactions as well as the concentration of enormous atmospheric species. As discussed in the response to Comment #3, these parameters for each individual alkene are with large uncertainty, and hence, this "bulk oxidant" method is an appropriate option. It should be noted that, the 25%, median, and 75% values of τ_{sCI} during nighttime under clean condition were 0.012 s, 0.017 s, and 0.021 s, respectively. Similarly, the 25%, median, and 75% values of τ_{OH} were 1.27×10^{-3} s, 1.73×10^{-3} s and 2.42×10^{-3} s, respectively. The variation of τ_{sCI} and τ_{OH} (roughly ± 50%) could be even smaller than the variation of the rate constants for different alkenes. So, the value of k_{app} may depend more on the mixing ratios of different alkenes.

Besides, the rate constants concerning the lifetime calculation for reactions of sCI with SO_2, H_2O, CO, NO_2, and NO as well as OH radical with VOCs, O_3, SO_2, CO, NO_2 and NO are listed below in Table S4.

Table R4 Rate constants for reactions of sCI and OH radical used for lifetime calculation

Compound	Reaction Constant (cm^{-3} s^{-1})*		Reference
Propylene	k_{OH}	3.19E-11	
Butadiene	k_{OH}	7.45E-11	
1-Butene	k_{OH}	3.53E-11	
Trans-2-Butene	k_{OH}	7.35E-11	
Cis-2-Butene	k_{OH}	6.37E-11	
Isoprene	k_{OH}	1.11E-10	
1-Pentene	k_{OH}	3.56E-11	
Trans-2-Pentene	k_{OH}	6.69E-11	
Cis-2-Pentene	k_{OH}	6.54E-11	
1-Hexene	k_{OH}	3.70E-11	
Butane	k_{OH}	2.19E-12	
Acetone	k_{OH}	1.80E-13	
Pentane	k_{OH}	3.63E-12	
Methyl Ethyl Ketone (MEK)	k_{OH}	1.11E-12	
Hexane	k_{OH}	1.77E-12	
Octane	k_{OH}	8.30E-12	
Nonane	k_{OH}	9.68E-12	
Decane	k_{OH}	1.08E-11	
Undecane	k_{OH}	1.29E-11	
Dodecane	k_{OH}	1.39E-11	MCMv3.3.1
Benzene	k_{OH}	1.16E-12	
Toluene	k_{OH}	6.13E-12	
Styrene	k_{OH}	5.80E-11	
m-Xylene	k_{OH}	2.31E-11	
p-Xylene	k_{OH}	1.43E-11	
o-Xylene	k_{OH}	1.36E-11	
Ethylbenzene	k_{OH}	7.00E-12	
1,3,5-Trimethylbenzene	k_{OH}	5.67E-11	
1,2,4-Trimethylbenzene	k_{OH}	3.25E-11	
1,2,3-Trimethylbenzene	k_{OH}	3.27E-11	
m-Ethyltoluene	k_{OH}	1.86E-11	
p-Ethyltoluene	k_{OH}	1.18E-11	
o-Ethyltoluene	k_{OH}	1.19E-11	
Propylbenzene	k_{OH}	6.30E-12	
Heptane	k_{OH}	6.86E-12	
Chloroform	k_{OH}	8.71E-14	
O_3	k_{OH}	5.75E-14	
SO_2	k_{OH}	1.37E-12	
CO	k_{OH}	5.64E-11	

NO_2	k_{OH}	3.65E-11	
NO	k_{OH}	1.81E-10	
SO_2	k_{sCI}	8.00E-13	(Mauldin et al., 2012)
H_2O	k_{sCI}	1.20E-15	(Newland et al., 2015)
CO	k_{sCI}	1.20E-15	MCMv3.3.1
NO_2	k_{sCI}	1.00E-15	MCMv3.3.1
NO	k_{sCI}	1.00E-14	MCMv3.3.1
sCI	$k_{sCI\text{-}dec}$	12.0 s	(Newland et al., 2015)

* The unit for rate constant is cm^{-3} s^{-1} if not specified.

References

Ahrens, J., Carlsson, P. T., Hertl, N., Olzmann, M., Pfeifle, M., Wolf, J. L., and Zeuch, T.: Infrared detection of Criegee intermediates formed during the ozonolysis of beta-pinene and their reactivity towards sulfur dioxide, Angew Chem Int Ed Engl, 53, 715-719, 10.1002/anie.201307327, 2014.

Almeida, J., Schobesberger, S., Kuerten, A., Ortega, I. K., Kupiainen-Maatta, O., Praplan, A. P., Adamov, A., Amorim, A., Bianchi, F., Breitenlechner, M., David, A., Dommen, J., Donahue, N. M., Downard, A., Dunne, E., Duplissy, J., Ehrhart, S., Flagan, R. C., Franchin, A., Guida, R., Hakala, J., Hansel, A., Heinritzi, M., Henschel, H., Jokinen, T., Junninen, H., Kajos, M., Kangasluoma, J., Keskinen, H., Kupc, A., Kurten, T., Kvashin, A. N., Laaksonen, A., Lehtipalo, K., Leiminger, M., Leppa, J., Loukonen, V., Makhmutov, V., Mathot, S., McGrath, M. J., Nieminen, T., Olenius, T., Onnela, A., Petaja, T., Riccobono, F., Riipinen, I., Rissanen, M., Rondo, L., Ruuskanen, T., Santos, F. D., Sarnela, N., Schallhart, S., Schnitzhofer, R., Seinfeld, J. H., Simon, M., Sipila, M., Stozhkov, Y., Stratmann, F., Tome, A., Troestl, J., Tsagkogeorgas, G., Vaattovaara, P., Viisanen, Y., Virtanen, A., Vrtala, A., Wagner, P. E., Weingartner, E., Wex, H., Williamson, C., Wimmer, D., Ye, P., Yli-Juuti, T., Carslaw, K. S., Kulmala, M., Curtius, J., Baltensperger, U., Worsnop, D. R., Vehkamaki, H., and Kirkby, J.: Molecular understanding of sulphuric acid-amine particle nucleation in the atmosphere, Nature, 502, 359-+, 10.1038/nature12663, 2013.

Jayne, J. T., Pöschl, U., Chen, Y.-m., Dai, D., Molina, L. T., Worsnop, D. R., Kolb, C. E., and Molina, M. J.: Pressure and Temperature Dependence of the Gas-Phase Reaction of SO3 with H2O and the Heterogeneous Reaction of SO3 with H2O/H2SO4 Surfaces, The Journal of Physical Chemistry A, 101, 10000-10011, 10.1021/jp972549z, 1997.

Kirkby, J., Curtius, J., Almeida, J., Dunne, E., Duplissy, J., Ehrhart, S., Franchin, A., Gagne, S., Ickes, L., Kuerten, A., Kupc, A., Metzger, A., Riccobono, F., Rondo, L., Schobesberger, S., Tsagkogeorgas, G., Wimmer, D., Amorim, A., Bianchi, F., Breitenlechner, M., David, A., Dommen, J., Downard, A., Ehn, M., Flagan, R. C., Haider, S., Hansel, A., Hauser, D., Jud, W., Junninen, H., Kreissl, F., Kvashin, A., Laaksonen, A., Lehtipalo, K., Lima, J., Lovejoy, E. R., Makhmutov, V., Mathot, S., Mikkila, J., Minginette, P., Mogo, S., Nieminen, T., Onnela, A., Pereira, P., Petaja, T., Schnitzhofer, R., Seinfeld, J. H., Sipila, M., Stozhkov, Y., Stratmann, F., Tome, A., Vanhanen, J., Viisanen, Y., Vrtala, A., Wagner, P. E., Walther, H., Weingartner, E., Wex, H., Winkler, P. M., Carslaw, K. S., Worsnop, D. R., Baltensperger, U., and Kulmala, M.: Role of sulphuric acid, ammonia and galactic cosmic rays in atmospheric aerosol nucleation, Nature, 476, 429-U477, 10.1038/nature10343, 2011.

Mauldin, R. L., III, Berndt, T., Sipilae, M., Paasonen, P., Petaja, T., Kim, S., Kurten, T., Stratmann, F., Kerminen, V. M., and Kulmala, M.: A new atmospherically relevant oxidant of sulphur dioxide, Nature, 488, 193-196, 10.1038/nature11278, 2012.

Newland, M. J., Rickard, A. R., Vereecken, L., Munoz, A., Rodenas, M., and Bloss, W. J.: Atmospheric isoprene ozonolysis: impacts of stabilised Criegee intermediate reactions with SO2, H2O and dimethyl sulfide, Atmospheric Chemistry and Physics, 15, 9521-9536, 10.5194/acp-15-9521-2015, 2015.

Sipila, M., Jokinen, T., Berndt, T., Richters, S., Makkonen, R., Donahue, N. M., Mauldin, R. L., III, Kurten, T., Paasonen, P., Sarnela, N., Ehn, M., Junninen, H., Rissanen, M. P., Thornton, J., Stratmann, F., Herrmann, H., Worsnop, D. R., Kulmala, M., Kerminen, V. M., and Petaja, T.: Reactivity of stabilized Criegee intermediates (sCIs) from isoprene and monoterpene ozonolysis toward SO2 and organic acids, Atmospheric Chemistry and Physics, 14, 12143-12153, 10.5194/acp-14-12143-2014, 2014.

Wine, P. H., Thompson, R. J., Ravishankara, A. R., Semmes, D. H., Gump, C. A., Torabi, A., and Nicovich, J. M.: Kinetics of the reaction OH + SO2 + M .fwdarw. HOSO2 + M. Temperature and pressure dependence in the fall-off region, The Journal of Physical Chemistry, 88, 2095-2104, 10.1021/j150654a031, 1984.

Yao, L., Garmash, O., Bianchi, F., Zheng, J., Yan, C., Kontkanen, J., Junninen, H., Mazon, S. B., Ehn, M., Paasonen, P., Sipila, M., Wang, M. Y., Wang, X. K., Xiao, S., Chen, H. F., Lu, Y. Q., Zhang, B. W., Wang, D. F., Fu, Q. Y., Geng, F. H., Li, L., Wang, H. L., Qiao, L. P., Yang, X., Chen, J. M., Kerminen, V. M., Petaja, T., Worsnop, D. R., Kulmala, M., and Wang, L.: Atmospheric new particle formation from sulfuric acid and amines in a Chinese megacity, Science, 361, 278-+, 10.1126/science.aao4839, 2018.

Yao, L., Fan, X., Yan, C., Kurten, T., Daellenbach, K. R., Li, C., Wang, Y., Guo, Y., Dada, L., Rissanen, M. P., Cai, J., Tham, Y. J., Zha, Q., Zhang, S., Du, W., Yu, M., Zheng, F., Zhou, Y., Kontkanen, J., Chan, T., Shen, J., Kujansuu, J. T., Kangasluoma, J., Jiang, J., Wang, L., Worsnop, D. R., Petaja, T., Kerminen, V. M., Liu, Y., Chu, B., He, H., Kulmala, M., and Bianchi, F.: Unprecedented Ambient Sulfur Trioxide (SO3) Detection: Possible Formation Mechanism and Atmospheric Implications, Environ Sci Technol Lett, 7, 809-818, 10.1021/acs.estlett.0c00615, 2020.